International Journal of Heat and Mass Transfer 78 (2014) 137–149

Contents lists available at ScienceDirect

International Journal of Heat and Mass Transfer

journal homepage: www.elsevier.com/locate/ijhmt

Effect of disjoining pressure (Π) on multi-scale modeling for evaporative liquid metal (Na) capillary

H. Yi [a], J. Tipton [a], K.D. Kihm [a,*], D.M. Pratt [b], A.D. Swanson [b], S. Rawal [c]

[a] The University of Tennessee, Knoxville, TN 37996, USA
[b] Air Force Research Laboratory, WPAFB, OH 45433, USA
[c] Lockheed Martin Space Systems Company, Denver, CO 80201, USA

A R T I C L E   I N F O

Article history:
Received 8 January 2014
Received in revised form 7 June 2014
Accepted 12 June 2014
Available online 17 July 2014

Keywords:
Liquid metal (sodium)
Evaporative thin film
Capillary meniscus
Disjoining pressure
Electronic degeneration
Work function

A B S T R A C T

This work presents a new multiscale model of an evaporating liquid metal capillary meniscus under nonequilibrium evaporation sustaining a nonisothermal interface. The primary investigation is elaborated on to examine the critical role of the disjoining pressure, which consists of both the traditional van der Waals component and a new electronic pressure component, for the case of liquid metals. The fully extended dispersion force is modeled along with an electronic disjoining pressure component that is unique to liquid metals attributing to their abundant free electrons. For liquid sodium (Na), as a favorable coolant for high temperature two-phase devices, the extended meniscus thin film model (sub-microscale) is coupled to a CFD model of the evaporating bulk meniscus (sub-millimeter scale). Two extreme cases are compared, i.e. with or without incorporation of the electronic disjoining pressure component. It is shown that the existence of electronic component of the disjoining pressure leads towards larger total capillary meniscus surface areas and larger net evaporative mass flow rates. Furthermore, the net evaporative mass flux in the bulk meniscus region is needed to be accounted for to obtain a true picture of the total capillary evaporation transport.

1. Introduction

Effective cooling schemes for high power density electronics, space-based nuclear reactors, hypersonic vehicle leading edges, and the like share a need for high temperature coolant operation and mass minimization. Liquid metal heat transport devices, such as heat pipes and capillary pumped loops, have the potential to meet these needs [1–4]. Their evaporative capacity and stability, however, depends upon accurate modeling of the evaporating extended meniscus region [5]. The interline or contact line region of an evaporating extended meniscus consists of three subregions in multiscales as schematically shown in Fig. 1: the adsorbed region where a disjoining pressure dominates the local atomic forces; the intrinsic or bulk meniscus region where the interfacial curvature governs the driving physics through surface tension; and the transition or thin-film region in between where both the disjoining pressure and the interfacial curvature share a comparable influence.

Liquid alkali metals, such as sodium, present complexities in the disjoining pressure models that have received little attention in the literature. In contrast to ordinary coolants such as water or pentane, the presence of abundant free electrons in liquid metals necessitates the additional "electronic pressure" or "electron degeneracy" contributions to the disjoining pressure [6]. This study seeks to address these modeling issues associated with liquid metal in the context of a physically realistic nonisothermal model of the evaporating thin film. To do so, the model must incorporate the near-wall micro/nano-scale phenomena as well as the macro-scale heat and mass transfer effects. Furthermore, a truly multiscale modeling is necessary to couple the submicroscale heat and mass transport in the thin film region and the macroscale transport in the bulk meniscus.

Visualization of a capillary evaporation experiment will be extremely difficult, if not impossible. Sodium lamps are a mature illumination technology that provides useful insight into the detrimental effects of sodium vapor. It is known that sodium vapor reacts chemically with silica (including Pyrex glass and Quartz) to form sodium silicate [7]. As a result, the glass container is chemically etched and develops orange/brown deposits which preclude visualization [8,9]. Commercial lighting applications have developed proprietary coatings of polycrystalline alumina which resist chemical attack but at the expense of transparency [10]. Sapphire tubing appears to be the only material available that can provide transparency and resistance to sodium vapor attack at high temperatures [11]. The

* Corresponding author. Tel.: +1 865 974 5292.
E-mail address: kkihm@utk.edu (K.D. Kihm).

http://dx.doi.org/10.1016/j.ijheatmasstransfer.2014.06.042
0017-9310/

Nomenclature

$a_{1,2,3}$	thin film boundary conditions
A	Hamaker constant [J]
B	disjoining pressure electronic component constant [N]
Ca	capillary number [Ca = $\mu_l u_0/\gamma$]
c_P	specific heat capacity at constant pressure [J/kg]
E_F	Fermi energy [eV]
h_{fg}	latent heat of evaporation [J/kg]
H	film thickness [m]
H_0	adsorbed film thickness [m]
i	imaginary number [$\sqrt{-1}$]
K	thin film curvature [m^{-1}]
m_e	electron mass [kg]
$\dot{m}''_{evp}$	evaporative mass flux [kg/s m^2]
M	molar mass [kg/mol]
$\dot{M}''$	nondimensionalized evaporative mass flux
N_e	valence electron number density [m^{-3}]
P	pressure [N/m^2]
q_e	electron charge [C]
q''	heat flux [W/m^2]
r	radial coordinate (cylindrical CS) [m]
R	pore radius [m]
R	universal gas constant [N m/K mol]
S	surface domain of integration
SA	surface area [m^2]
T	temperature [K]
T^*	nondimensional interfacial temperature
ΔT	liquid overheat [K]
u	horizontal velocity [m/s]
v	vertical velocity [m/s]
v_e	plasma frequency of an electron gas [Hz]
x	axial coordinate (Cartesian CS) [m]
y	vertical coordinate (Cartesian CS) [m]
z	horizontal coordinate (cylindrical CS) [m]

Greek Symbols

α	evaporation coefficient
γ	surface tension [N/m]
ε_0	permittivity of free space [s^4 A^2/m^3 kg]
ε_1	relative permittivity of container
ε_2	relative permittivity of vapor
ε_3	relative permittivity of liquid thin film
η	nondimensional axial coordinate [$\eta = x/x_0$]
θ	radial coordinate (cylindrical CS) [rad]
θ	nondimensional film thickness [$\theta(\eta) = H/H_0$]
κ	ratio of evaporative interfacial resistance to conductive resistance
κ_n	electronic disjoining pressure work function parameter
λ	thermal conductivity [W/m K]
μ	viscosity[N s/m^2]
ξ	nondimensionalized distance mapped for Chebyshev polynomials
Π	disjoining pressure [N/m^2]
$\bar{\Pi}$	nondimensional disjoining pressure [$\bar{\Pi} = \Pi/\Pi_0$]
ρ	density [kg/m^3]
σ	optical conductivity [S/m]
τ	relaxation time [s]
χ	electronic disjoining pressure boundary condition
ω	frequency [rad/s]
ω_e	plasma frequency of an electron gas [rad/s]
ω_n	electromagnetic wave frequency [rad/s]

Subscripts

0	reference state
A	dispersion component of the disjoining pressure
B	electronic component of the disjoining pressure
lv	liquid/vapor interface
l	liquid
tf	thin film
v	vapor
w	wall

anisotropic nature of this crystalline material, however, makes it prone to cracks and sealing problems. Indeed, experimental visualization of liquid sodium capillary evaporation will prove difficult.

2. Background

Previous studies have addressed numerical heat and mass transfer solutions to steady extended meniscus evaporation where

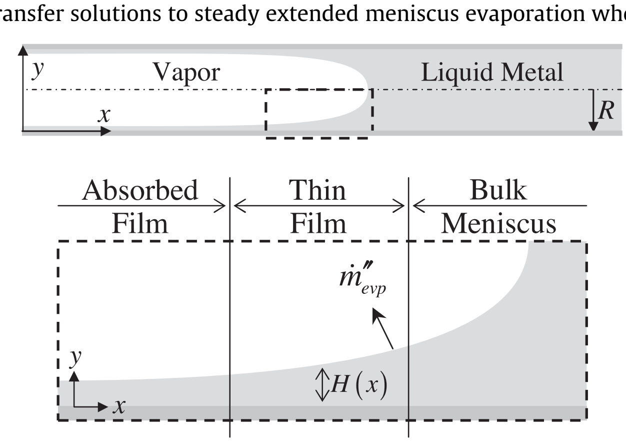

Fig. 1. Schematic of a cylindrical capillary geometry identifying the distinct regions of the extended evaporating meniscus.

a static interline region continually replenished by fluid from the intrinsic meniscus. Wayner and Schonberg [12] developed a governing equation for the film height of a symmetric meniscus as a function of distance between two feed ports. Their development draws upon the pioneering thin film experiments of Derjaguin [13], Schrage's [14] relationship for net mass flux across a liquid/vapor interface, and the evaporating extended meniscus models of Potash and Wayner [15] and Wayner et al. [16]. Later, Hallinan et al. [17] introduced new nondimensional variables and used an explicit Runge–Kutta numerical solution procedure to solve the more complicated (and realistic) case of extended meniscus evaporation under nonisothermal interface conditions.

For the case of neutral atoms and non-polar molecules, London dispersion forces act as a prevailing component of the disjoining pressure in thin films. Dzyaloshinskii, Lifshitz, and Pitaevskii (DLP) used quantum electrodynamics to derive the first general theory of van der Waals forces [18], which includes the London dispersion force. Previous studies [5,19–21] have utilized only approximations to the full DLP theory, so called Hamaker approximations that were valid as long as (a) dielectric materials were used, i.e., for non-metallic coolants with no free electrons presented, (b) the film thicknesses were much greater or less than "the wavelengths which characterize the absorptions spectra of the given bodies", and (c) a temperature requirement was met to be in a moderate range [18]. The case of a high temperature, liquid